

# Characterization of Lipid-Rich Aortic Plaques by Intravascular Photoacoustic Tomography

## Ex Vivo and In Vivo Validation in a Rabbit Atherosclerosis Model With Histologic Correlation



Jian Zhang, PhD,\* Sihua Yang, PhD,\* Xuanrong Ji, PhD,\* Quan Zhou, MD,† Da Xing, PhD\*

### ABSTRACT

**BACKGROUND** Histologic studies have demonstrated that lipid content and its spatial distribution is related to plaque vulnerability. However, in vivo imaging is still limited. Photoacoustic imaging may provide novel in vivo insights into these lipid-rich plaques.

**OBJECTIVES** This study sought to examine whether intravascular photoacoustic tomography (IVPAT) allows localization and quantification of lipid content in atherosclerotic plaques.

**METHODS** Rabbits fed with a high-fat/high-cholesterol diet served as the atherosclerotic model. Catheter-based IVPAT was used to evaluate pixel-based lipid relative concentration (LRC) of the vessel wall. The aorta of 4 groups of rabbits ( $n = 12$ ) were examined ex vivo with IVPAT after 0, 5, 10, and 15 weeks of a high-fat diet, respectively. Six rabbits underwent 3-dimensional (3D) IVPAT after 20 weeks of the high-fat diet. Three rabbits were examined in vivo using IVPAT without interruption of blood flow. Concentration-based lipid map and quantitative index were calculated. For subsequent histologic correlation, all specimens were evaluated with Oil Red O staining.

**RESULTS** Cross-sectional LRC maps allowed visualization of concentration and depth information of lipid content in the atherosclerotic plaques. Lipid accumulation within plaque, assessed by the maximum LRC, mean LRC, and high lipid content area correlated to duration of a high-fat diet. Three-dimensional LRC maps enabled overall evaluation of focal plaques in an intact explanted aorta including spatial and structural features. In vivo-obtained LRC maps accurately showed the structure of lipid core with high contrast. Ex vivo and in vivo IVPAT results were highly consistent with histological results.

**CONCLUSIONS** In an animal model, IVPAT allowed characterization of spatial and quantitative features of lipid-rich plaques. (J Am Coll Cardiol 2014;64:385-90) © 2014 by the American College of Cardiology Foundation

Historical studies have demonstrated that the primary cause of acute cardiovascular events is the rupture of atherosclerotic plaques. Lipid content and its distribution within the plaque influence the propensity of plaques to disrupt flow (1,2). Based on this hypothesis, a series of pivotal clinical trials have proven that lipid-lowering therapy

can reduce cardiovascular morbidity and mortality (3,4). However, current intravascular imaging techniques have inherent limitations for characterizing lipid content within atherosclerotic plaques. Thus, there is a need for a method that enables an in situ quantitative and spatial characterization of lipid content in the vessel wall (5).

From the \*Ministry of Education Key Laboratory of Laser Life Science and Institute of Laser Life Science, College of Biophotonics, South China Normal University, Guangzhou, Guangdong Province, China; and the †Medical Imaging Center, First Affiliated Hospital of Jinan University, Guangzhou, Guangdong Province, China. This research was supported by grants from the National Basic Research Program of China (2010CB732602; 2011CB910402), the Program for Changjiang Scholars and Innovative Research Team in University (IRT0829), and the National Natural Science Foundation of China (61361160414; 61331001; 81127004; 11104087). The authors have reported that they have no relationships relevant to the contents of this paper to disclose.

Manuscript received January 6, 2014; revised manuscript received April 28, 2014, accepted April 29, 2014.



**ABBREVIATIONS  
AND ACRONYMS**

**HFC** = high fat/high cholesterol

**IVPAT** = intravascular photoacoustic tomography

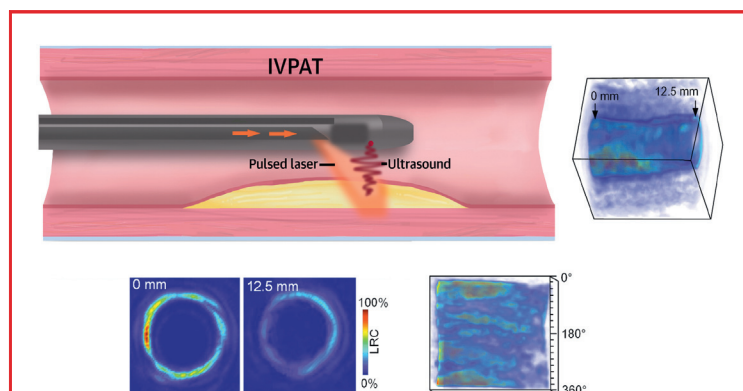
**IVUS** = intravascular ultrasound

**LRC** = lipid relative concentration

**3D** = 3-dimensional

As a hybrid imaging technique, photoacoustic tomography provides the volumetric images of tissues with optical contrast and ultrasonic resolution by reconstructing the detected photoacoustic signal (6-8). Intravascular photoacoustic tomography (IVPAT) has great potential for meticulous in vivo examinations of atherosclerotic changes in the vessel wall. Previous studies have demonstrated feasibility of plaque visualization (9-11) with this modality. More recent work has focused on detecting lipid-rich components in atherosclerotic plaques (12,13). However, quantitative and spatial characterization of the lipid content has been incomplete.

SEE PAGE 391



Comparison of Intravascular Imaging Techniques for Characterization of Atherosclerotic Plaques

| Physical Property           | Technique        | Resolution      | Penetration | Histological or Physiological Targets   | Specialized Lipid Imaging Capability |
|-----------------------------|------------------|-----------------|-------------|---|--------------------------------------|
| Acoustic                    | IVUS             | 100 $\mu$ m     | 8-10 mm     | Arterial wall remodeling, lipid core (echolucent core) and plaque area              | NA                                   |
|                             | IVUS-RF analysis | 100-200 $\mu$ m | 8-10 mm     | Plaque composition (fibrous, fibro-fatty, calcified tissues and calcified necrosis) | Poor                                 |
| Light scattering/absorbance | OCT              | 4-20 $\mu$ m    | 1-2 mm      | Thin fibrous cap, macrophages and thrombosis  | NA                                   |
|                             | NIRS             | NA              | 1-2 mm      | Lipid core  | Good                                 |
| Photoacoustic               | IVPAT            | 100 $\mu$ m     | 2-4 mm      | Plaque morphology, lipid core   | Good                                 |

**CENTRAL ILLUSTRATION** Characterization of Lipid-Rich Aortic Plaques by IVPAT

Intravascular photoacoustic tomography (IVPAT), a catheter-based hybrid imaging modality, permits in situ meticulous examination of atherosclerotic lesions. IVPAT can directly show the lipid relative concentration (LRC) maps (cross-sectional map, longitudinal 3-dimensional map or en-face 3-dimensional map) of plaques. From these maps, comprehensive and quantitative indexes of lipid are measurable and have excellent correlation with histological measurement. The comparison between IVPAT and several clinical available intravascular imaging techniques are given in the table portion of the illustration. IVUS = intravascular ultrasound; NA = not applicable; NIRS = near-infrared spectroscopy; OCT = optical coherence tomography; RF = radiofrequency.

In an animal model, we therefore examined the feasibility of a catheter-based IVPAT imaging platform to construct 3-dimensional (3D), concentration-based maps of lipid components in atherosclerotic plaques (Central Illustration). A series of ex vivo and in vivo experiments were performed with subsequent histologic correlation.

**METHODS**

**ANIMALS.** The Animal Study Committee at South China Normal University College of Biophotonics in Guangdong, China, approved all animal procedures. New Zealand white rabbits (male, age 3 months, weight 2.3 to 2.8 kg) served as the experimental model of atherosclerosis. Atherosclerotic changes were induced with a high-fat/high-cholesterol (HFC) diet (97% normal chow, 2% lard, and 1% cholesterol).

**IVPAT.** Figure 1 describes the experimental setup of the IVPAT system and the lipid imaging process. The current system had an approximate 100- $\mu$ m axial resolution, an approximate 380- $\mu$ m transverse resolution and more than 2 mm of imaging depth (Online Fig. 1). The system was operated via a custom-made LabVIEW program (National Instruments, Austin, Texas). MATLAB software (Mathworks, Natick, Massachusetts) was used for image construction and index measurement.

**EXPERIMENTAL PROTOCOL.** In the first set of experiments, IVPAT was used to monitor the development/progression of induced atherosclerosis in 4 groups of rabbits (n = 12) after 0, 5, 10, or 15 weeks of the HFC diet. In subsequent experiments, intact aortas of 6 rabbits were imaged over the entire length after 20 weeks of HFC feeding to obtain 3D lipid relative concentration (LRC) maps. In these experiments, imaging was performed ex vivo, after the animal was sacrificed. Lastly, the aortas of 3 rabbits were examined in vivo at 20 weeks (n = 1) or 25 weeks (n = 2) with IVPAT and magnetic resonance imaging, before sacrificing the animal, as shown in Figure 2. (See the Online Appendix for additional information.)

Following IVPAT imaging, all specimens were evaluated with en-face Oil Red O staining or cross-sectional Oil Red O staining. Maximum LRC, mean LRC, and high lipid content area in the LRC maps were measured by analyzing their entire units with MATLAB. High lipid content area of histological examination was quantified using Image Pro plus software (Media Cybernetics, Rockville, Maryland). A detailed description of the lipid-imaging process and the experimental protocol is provided in the Online Appendix.

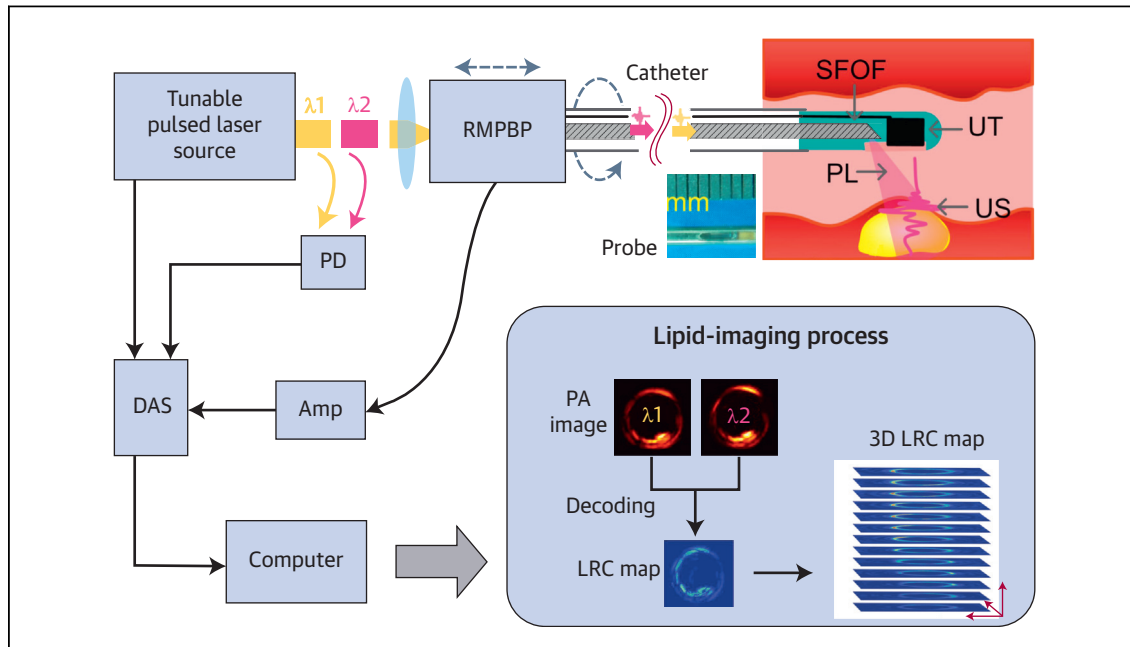


**FIGURE 1** Schematic of the Catheter-Based IVPAT Imaging Platform and the Lipid-Imaging Process

Dual-wavelength ( $\lambda_1$  and  $\lambda_2$ ) pulsed laser (PL) generated from a tunable pulsed laser source were coupled into a side-fire optical fiber (SFOF), which was integrated with an ultrasonic transducer (UT). The outer diameter of the intravascular photoacoustic tomography (IVPAT) probe was 1.8 mm, as shown in the probe photograph. The PL was directed to excite the vascular wall to generate ultrasonic signals (US), which were detected by the UT. The detected US were coupled out of the catheter, amplified by an amplifier (Amp) and acquired by a data acquisition system (DAS), then recorded on a computer and finally reconstructed into a photoacoustic (PA) image. A photo diode (PD) was used to monitor the laser intensity. A custom-made rotating motor and pullback platform (RMPBP) was used to achieve cross-sectional imaging and 3-dimensional (3D) imaging. The lipid relative concentration (LRC) map was extracted by decoding dual-wavelength PA images and is shown as a color-calibrated cross-sectional image or 3D image.

**STATISTICAL ANALYSIS.** Data are presented as mean  $\pm$  SD. Correlation between IVPAT and histology was tested with linear regression analysis using Origin (OriginLab Corporation, Northampton, Massachusetts). Bland-Altman tests (14) were performed to determine the agreement between them with GraphPad Prism (GraphPad Software, La Jolla, California).

**RESULTS**

Our first goal was to assess diet-induced atherosclerosis development or progression as monitored by ex vivo IVPAT versus histology. **Figure 3** shows representative LRC maps at the 4 time points (after 0, 5, 10, and 15 weeks on the HFC diet), respectively. **Figure 3A** demonstrates a low lipid aortic

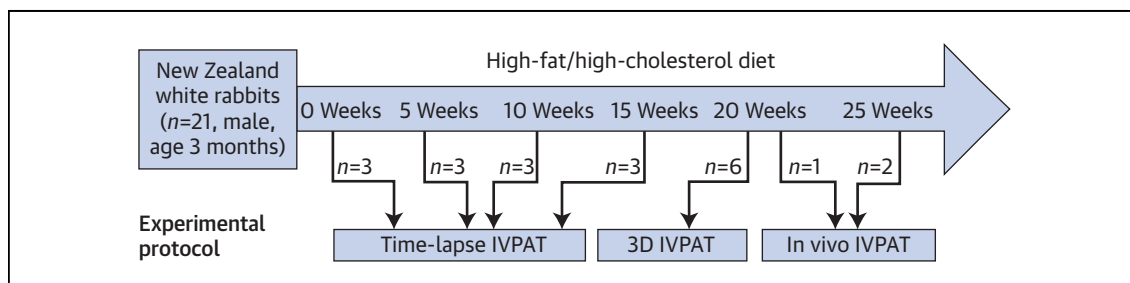


**FIGURE 2** Experimental Protocol

Experimental protocol illustrating the series of IVPAT imaging experiments performed using rabbit aortas as the atherosclerosis model. Abbreviations as in **Figure 1**.

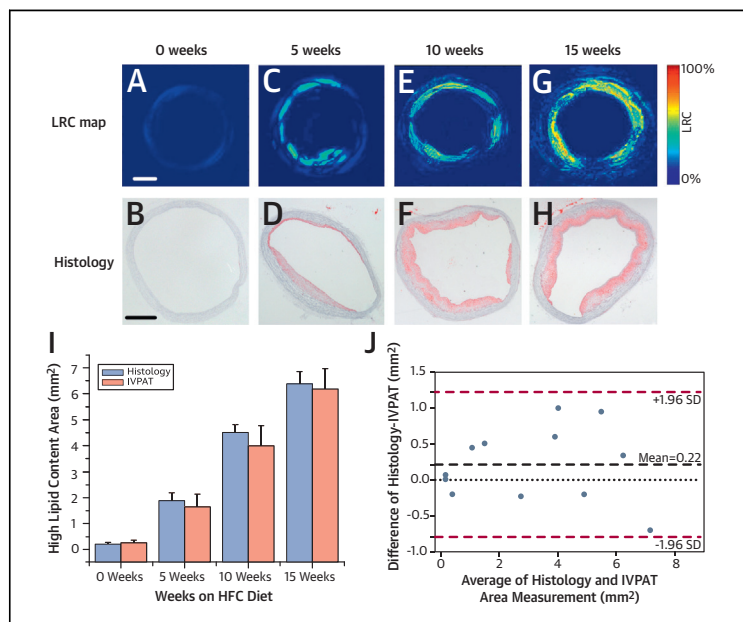


**FIGURE 3** Diet-Induced Atherosclerosis Development/Progression Monitored by Ex Vivo IVPAT Versus Histology

Representative results of lipid accumulating and arterial wall remodeling in relation to the duration of high-fat diet monitored by IVPAT and histology: 0 weeks (A, B); 5 weeks (C, D); 10 weeks (E, F); or 15 weeks (G, H). Normalized image intensity of LRC maps enabled a quantitative comparison. The scale bar is 1 mm. (I) High lipid area in the aortic wall, measured by IVPAT and histology, was plotted against duration of high-fat diet. (J) Bland-Altman tests for all results (n = 12). HFC = high fat/high cholesterol; other abbreviations as in Figure 1.

wall of a healthy rabbit in which the maximum LRC was about 30%. As exemplified by other LRC maps (Figs. 3C, 3E, and 3G), the high lipid content area (LRC  $\geq$ 30%) significantly expanded from nearly 0 to  $6.19 \pm 0.81$  mm<sup>2</sup> (Fig. 3I) after 15 weeks of the HFC diet. Meanwhile, the maximum LRC within the intima increased up to  $90.7 \pm 6.5\%$ . The mean LRC of the intima increased from  $6.24 \pm 2.5\%$  to  $39.6 \pm 5.3\%$ . However, the mean LRC in the adventitia remained at a stable level at around 6% (Table 1).

**TABLE 1** Maximum LRC and Mean LRC Changed With the Time of HFC Diet Feeding

| Location   |      | Time            |                  |                  |                 |
|------------|------|-----------------|------------------|------------------|-----------------|
|            |      | 0 Weeks         | 5 Weeks          | 10 Weeks         | 15 Weeks        |
| Intima     | Max  | $30.7 \pm 5.40$ | $63.3 \pm 14.30$ | $86.65 \pm 7.80$ | $90.7 \pm 6.50$ |
|            | Mean | $6.24 \pm 2.50$ | $10.43 \pm 6.30$ | $22.35 \pm 7.80$ | $39.6 \pm 5.30$ |
| Adventitia | Max  | $29.5 \pm 1.90$ | $33.2 \pm 3.60$  | $37.5 \pm 2.80$  | $35.8 \pm 2.60$ |
|            | Mean | $5.52 \pm 1.30$ | $6.12 \pm 2.10$  | $6.47 \pm 3.70$  | $6.51 \pm 3.20$ |

Values are mean  $\pm$  SD.  
HFC = high fat/high cholesterol; LRC = lipid relative concentration.

Histology (Figs. 3B, 3D, 3F, and 3H) demonstrated the same characteristics. Both the linear regression analysis ( $r = 0.978$ ,  $p < 0.0001$ ) and the Bland-Altman tests (Fig. 3J) verified excellent correlation between IVPAT and histology.

Next, we sought to assess the characterization of entire length atherosclerotic aortas by ex vivo 3D IVPAT. Longitudinal 3D LRC map (Fig. 4A, Online Video 1) enabled an overall evaluation of an intact rabbit aorta affected by large-area plaques after 20 weeks of HFC feeding. Corresponding en-face 3D LRC map (Fig. 4B, Online Video 2) demonstrated a positive relationship between the lipid accumulation and the intima thickening. The en-face histology (Fig. 4C) verified the nonuniform distribution. Furthermore, cross-sectional LRC maps (Figs. 4D and 4E) could visualize lipid components within plaques with content and depth information. Linear regression analysis ( $r = 0.972$ ,  $p < 0.0001$ ) as well as Bland-Altman tests of the other 3 aortic segments (Fig. 4F) demonstrated a high degree of coherency between 3D IVPAT and continuous frozen sections (Online Fig. 4).

**LIPID IMAGING BY IN VIVO IVPAT.** Magnetic resonance imaging visualizes plaque morphology (Figs. 5A, 5D, and 5G), but it was insufficient to specify lipid content within plaques. IVPAT obtained high-contrast LRC maps at the same imaging planes (Figs. 5B, 5E, and 5H), which simultaneously showed content and distribution of lipid within the plaques. The whole boundary of the lipid-rich intima could be distinguished, which matched well with the histology (Figs. 5C, 5F, and 5I). Further measurements demonstrated that all 3 intima had  $>95\%$  maximum LRC and  $>40\%$  mean LRC. Although the blood flow was kept during the data acquisition, IVPAT probe could be located by x-ray (Fig. 5J). The relative error between IVPAT and histology was approximately 10% (Fig. 5K).

## DISCUSSION

Our data demonstrate the feasibility of in vivo IVPAT for characterization of spatial and quantitative features of lipid-rich plaques. Compared with other intravascular plaque imaging modalities, the advantage of IVPAT is the combined utilization of light and sound wave features for image generation.

The theoretical advantage of IVPAT can be derived from the limitations of other imaging modalities, specifically intravascular ultrasound (IVUS, sound wave based) and near-infrared spectroscopy (light wave based) (15). Grayscale IVUS has a high imaging depth that enables a full-field evaluation of

plaques with large lipid cores. And virtual histology IVUS can distinguish plaque components. However, detailed assessment of lipid content is limited (16,17). Near-infrared spectroscopy provides several valuable indexes for evaluating lipid content (18,19). However, near-infrared spectroscopy is an en-face imaging mode that only enables the evaluation of lipid from a 2-dimensional image plane (endothelial surface), without depth information.

As a hybrid imaging technique, IVPAT integrates the advantages of optical contrast and ultrasonic resolution (20), which can simultaneously demonstrate the spatial distribution and relative concentration of lipid content in atherosclerotic plaques along entire vessel segments. Furthermore, the unique combination of the optical and ultrasonic components suggests prospective multiple-imaging modalities with IVUS or optical coherence tomography (21) for comprehensively evaluating plaque structures (e.g., calcification, arterial wall remodeling, and fibrous cap).

**STUDY LIMITATIONS.** First, the transverse resolution was not satisfactory, because the laser spot of this optical fiber was relatively large. Second, the repetition frequency of the laser used was 10 Hz, so that

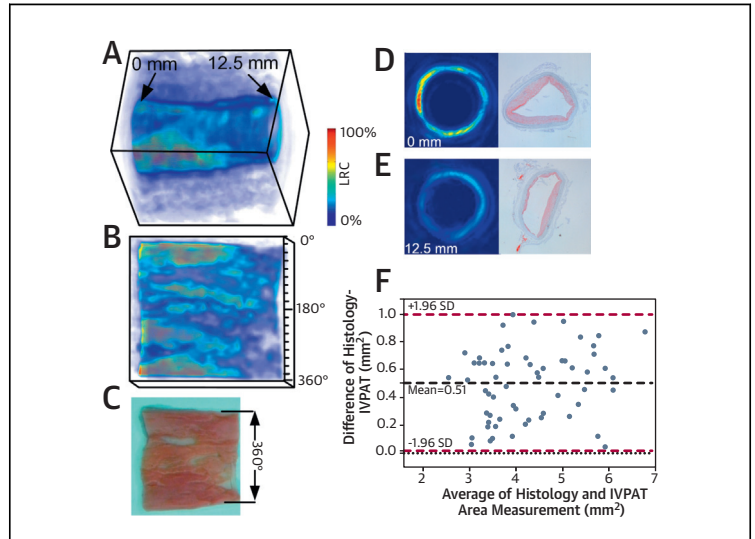


**FIGURE 4** 3D Imaging of Lipid Within Intact Atherosclerotic Aortas by IVPAT

(A) A longitudinal 3D LRC map of an intact atherosclerotic aorta (20 weeks HFC diet feeding). (B) Corresponding en-face 3D LRC map viewed from inside of the aorta over a 360° field. (C) En-face histology. (D and E) Cross-sectional LRC maps and corresponding histology located at 0 mm and 12.5 mm. (F) Bland-Altman tests of high lipid content area (n = 58) measured from cross-sectional LRC maps and histology. See [Online Videos 1 and 2](#). Abbreviations as in [Figures 1 and 3](#).

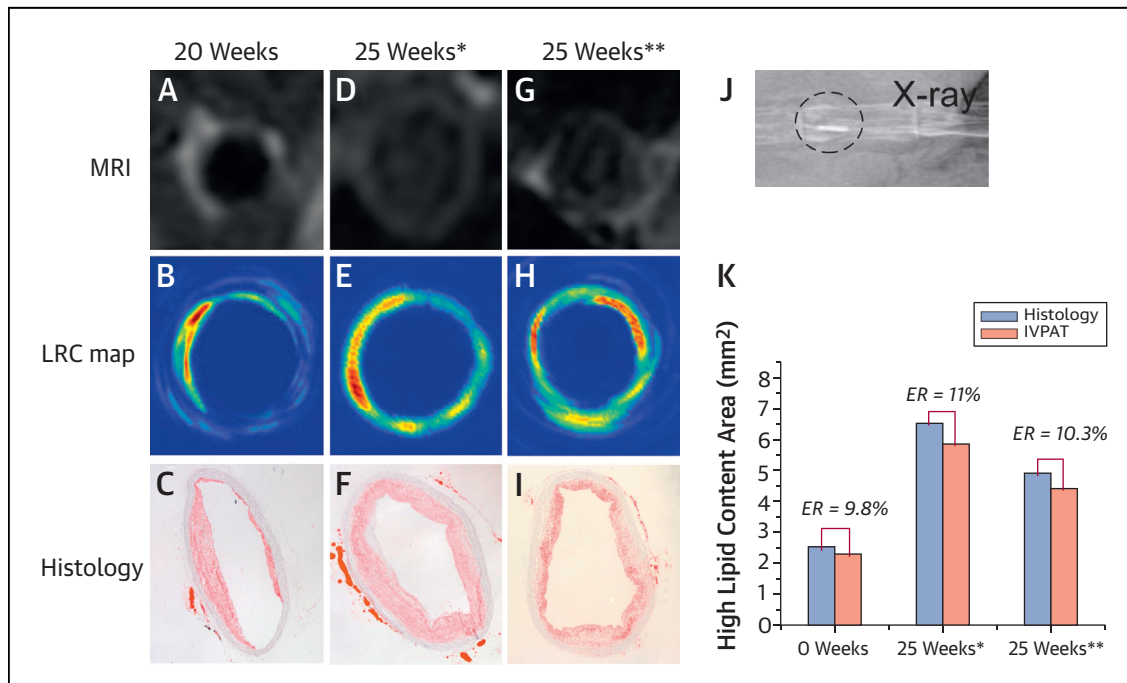


**FIGURE 5** In Vivo IVPAT Imaging of Lipid in the Atherosclerotic Plaques

Magnetic resonance imaging (MRI) results, LRC map, and histological image of 3 rabbits in vivo examined with in vivo IVPAT after 20 weeks (A to C) or 25 weeks (D to F, G to I) HFC diet feeding. (J) X-ray image showed the location of IVPAT probe within the rabbit aorta. (K) Comparison of the high lipid content area measured by IVPAT and histology. ER = relative error; other abbreviations as in [Figures 1 and 3](#).

the in vivo 3D visualization of lipid content has not been achieved. The in vivo IVPAT results showed slight dislocation, which we thought was caused by the heartbeat-driven vascular deformation during the ultrasonic signal acquisition. Third, current results were based on rabbit atherosclerotic plaques, and further studies should be undertaken on human plaques to assess the capabilities and potential benefits of IVPAT.

## CONCLUSIONS

Our data demonstrate feasibility of in vivo IVPAT for characterization of spatial and quantitative features of lipid-rich plaques and encourages further development of IVPAT for basic science research and clinical diagnosis of atherosclerosis.

**ACKNOWLEDGMENTS** The authors are grateful to Minjie Liang and Junqing Yang for their help with the statistical and histological methodologies.

**REPRINT REQUESTS AND CORRESPONDENCE:** Drs. Da Xing or Sihua Yang, South China Normal University, College of Biophotonics, No. 55, Zhongshan Road, Guangzhou, Guangdong Province 510631, China. E-mail: [xingda@scnu.edu.cn](mailto:xingda@scnu.edu.cn) OR [yangsh@scnu.edu.cn](mailto:yangsh@scnu.edu.cn).

## PERSPECTIVES

**COMPETENCY IN MEDICAL KNOWLEDGE 1:** The formation of lipid-rich arterial plaque is a key event in the progression of atherosclerosis, and both lipid content and distribution within the plaque contribute to plaque stability.

**COMPETENCY IN MEDICAL KNOWLEDGE 2:** Delineation of the relative lipid concentration map by high resolution, dual-wavelength intravascular photoacoustic tomography (IVPAT) is a quantitative method for characterization of the morphology of immature, proliferative atherosclerotic plaques.

**TRANSLATIONAL OUTLOOK 1:** Further studies of IVPAT are needed to assess its accuracy for the assessment of more mature atherosclerotic plaques complicated by calcification and thrombus formation.

**TRANSLATIONAL OUTLOOK 2:** Additional studies are needed to determine whether combining IVPAT with other imaging techniques such as optical coherence tomography and intravascular ultrasound can accurately assess features associated with plaque vulnerability and predict clinical ischemic events.

## REFERENCES

- Virmani R, Burke AP, Farb A, Kolodgie FD. Pathology of the vulnerable plaque. *J Am Coll Cardiol* 2006;47 Suppl 8:C13-8.
- Hamm CW, Braunwald E. A classification of unstable angina revisited. *Circulation* 2000;102:118-22.
- Nissen SE, Tuzcu EM, Schoenhagen P, et al., for the REVERSAL Investigators. Effect of intensive compared with moderate lipid-lowering therapy on progression of coronary atherosclerosis: a randomized controlled trial. *JAMA* 2004;291:1071-80.
- Herder M, Arntzen KA, Johnsen SH, Eggen AE, Mathiesen EB. Long-term use of lipid-lowering drugs slows progression of carotid atherosclerosis the Tromso study 1994 to 2008. *Arterioscler Thromb Vasc Biol* 2013;33:858-62.
- Bourantas CV, Garcia-Garcia HM, Naka KK, et al. Hybrid intravascular imaging: current applications and prospective potential in the study of coronary atherosclerosis. *J Am Coll Cardiol Img* 2013;61:1369-78.
- Burgholzer P, Grün H, Sonnleitner A. Photoacoustic tomography: sounding out fluorescent proteins. *Nat Photonics* 2009;3:378-9.
- Razansky D, Distel M, Vinegoni C, et al. Multispectral opto-acoustic tomography of deep-seated fluorescent proteins in vivo. *Nat Photonics* 2009;3:412-7.
- Wang LV, Hu S. Photoacoustic tomography: in vivo imaging from organelles to organs. *Science* 2012;335:1458-62.
- Hsieh BY, Chen SL, Ling T, Guo LJ, Li PC. Integrated intravascular ultrasound and photoacoustic imaging scan head. *Opt Lett* 2010;35:2892-4.
- Jansen K, van der Steen AF, van Beusekom HM, Oosterhuis JW, van Soest G. Intravascular photoacoustic imaging of human coronary atherosclerosis. *Opt Lett* 2011;36:597-9.
- Li X, Wei W, Zhou Q, et al. High frequency intravascular photoacoustic (IVPA) imaging for differentiating arterial wall layered structures. *Proc SPIE* 2012;8207:820746.
- Wang B, Karpiouk A, Yeager D, et al. Intravascular photoacoustic imaging of lipid in atherosclerotic plaques in the presence of luminal blood. *Opt Lett* 2012;37:1244-6.
- Qin H, Zhou T, Yang S, Chen Q, Xing D. Gadolinium (III)-gold nanorods for MRI and photoacoustic imaging dual-modality detection of macrophages in atherosclerotic inflammation. *Nanomedicine* 2013; 8:1611-24.
- Bland MJ, Altman DG. Statistical methods for assessing agreement between two methods of clinical measurement. *Lancet* 1986;1:307-10.
- Honda Y, Fitzgerald PJ. Frontiers in intravascular imaging technologies. *Circulation* 2008;117:2024-37.
- Nissen SE, Yock P. Intravascular ultrasound: novel pathophysiological insights and current clinical applications. *Circulation* 2001;103:604-16.
- Nair A, Kuban BD, Tuzcu EM, Schoenhagen P, Nissen SE, Vince DG. Coronary plaque classification with intravascular ultrasound radiofrequency data analysis. *Circulation* 2002;106:2200-6.
- Caplan JD, Waxman S, Nesto RW, Muller JE. Near-infrared spectroscopy for the detection of vulnerable coronary artery plaques. *J Am Coll Cardiol* 2006;47 Suppl 8:C92-6.
- Kini AS, Baber U, Kovacic JC, et al. Changes in plaque lipid content after short-term intensive versus standard statin therapy: the YELLOW trial (reduction in yellow plaque by aggressive lipid-lowering therapy). *J Am Coll Cardiol* 2013;62:21-9.
- Li PC, Wei CW, Sheu YL. Subband photoacoustic imaging for contrast improvement. *Opt Express* 2008;16:20215-26.
- Yabushita H, Bouma BE, Houser SL, et al. Characterization of human atherosclerosis by optical coherence tomography. *Circulation* 2002; 106:1640-5.

**KEY WORDS** atherosclerosis, histological imaging, intravascular photoacoustic tomography, lipid

**APPENDIX** For supplemental information, figures, and accompanying videos and legends, please see the online version of this article.